

# Neutron Star Mergers and the Quark Matter Equation of State

Grant J. Mathews<sup>1,\*</sup>, Atul Kedia<sup>1,†</sup>, Hee Il Kim<sup>2,‡</sup>, and In-Saeng Suh<sup>1,3,§</sup>

<sup>1</sup>Department of Physics and Astronomy, Center for Astrophysics, University of Notre Dame, Notre Dame, IN 46556, USA

<sup>2</sup>Center for Quantum Spacetime, Sogang University, Seoul 04107, Korea

<sup>3</sup>Center for Research Computing, University of Notre Dame, Notre Dame, IN 46556, USA

**Abstract.** As neutron stars merge they can approach very high nuclear density. Here, we summarized recent results for the evolution and gravitational wave emission from binary-neutron star mergers using a variety of nuclear equations of state with and without a crossover transition to quark matter. We discuss how the late time gravitational wave emission from binary neutron star mergers may possibly reveal the existence of a crossover transition to quark matter.

## 1 Introduction

In recent work [1] we have explored the effects of a crossover transition to quark matter on the emergent gravitational waves from binary neutron star mergers. In this paper we summarize that work and other efforts toward unraveling the effects of the formation of quark-matter during neutron-star mergers. Neutron stars (NSs) and NS binaries can probe the equation of state (EOS) at supra-nuclear densities (for recent reviews see Refs. [2, 3]). Indeed, the detection of gravitational waves (GWs) from the GW170817 event by the LIGO-Virgo Collaboration [4, 5] provided new insights into the properties of neutron-star matter [6]. Beyond that, determinations of NS masses and radii by the NICER mission also constrain the EOS of nuclear matter [7–9]. Tidal effects can be inferred from the signal in ground-based GW observatories [10–12]. In the LIGO-Virgo events tidal deformability ( $\Lambda$ ) of a NS of mass  $M = 1.4 M_{\odot}$  have also been inferred  $\Lambda_{1.4} < 800$  at (90% C.L.) for a low-spin prior [4] and the radius constraint for a  $M = 1.4 M_{\odot}$  NS was deduced to be  $R_{1.4} < 13.6$  km. Subsequently, this has been further constrained to be  $R_{1.4} = 11.9 \pm 1.4$  km [5]. Also, newer constraints on the maximum NS mass and a lower limit of the tidal deformability were also inferred [13, 14]. Adding the requirement that the equation of state asymptotically approach the regime of perturbative QCD [14–19], leads to constraints on the radius of a maximum-mass NS of  $R_{\max} < 13.6$  km and  $\Lambda_{1.4} > 120$  [14]. It has also been shown that an EOS with a phase transition can imply  $8.53 \text{ km} < R_{1.4} < 13.74 \text{ km}$  and  $\Lambda_{1.4} > 35.5$  at the  $3 \sigma$  level [13].

There is currently much interest in the fact that a phase transition in the EOS can produce a variety of dynamical collapse patterns (cf. [20]). As explained below, such changes in the

---

\*e-mail: gmathews@nd.edu

†e-mail: atulkedia93@gmail.com

‡e-mail: khizetta@sogang.ac.kr

§e-mail: isuh@nd.edu

EOS can produce a shift of the maximum peak frequency ( $f_{peak}$  (sometimes denoted as  $f_2$ ) in the detected power spectral density (PSD) [21–23]. Such a shift can violate the universal relation between  $f_{peak}$  and tidal deformability that has been noted for pure hadronic EOSs [24]. However, an EOS with a phase transition may not conform to the same empirical universal relations [25–29]. Hence, an observed shift might indicate the formation of quark matter. This conclusion, however, is model dependent (e.g. [30, 31]) and also depends upon the duration of merger remnant [20, 32, 33].

A number of recent works have discussed EOS effects on the GW signal. Some of them have also considered the formation of quark matter [20–22, 31–35]. Most of these studies, however, have considered a first-order phase transition. In this case a mixed quark-hadron phase forms which can remove pressure support leading to a prompt collapse. However, since the strength of the order parameter for the QCD phase transition is not known, a simple crossover or a weakly first-order transition is possible [36–40]. The pressure in the regime of the crossover could be large compared to a hadronic or a first-order transition. This could extend the postmerger phase. Hence, an observation of a long-duration post-merger GW event, could possibly indicate both the order of the transition and the coupling strength of quark-matter in the crossover regime [1].

In Ref. [1] we examined the crossover to the formation of quark-gluon plasma during the postmerger and demonstrated that the GW signal from the postmerger phase is indeed sensitive to the quark-matter EOS. It was shown that the properties of quark matter in the non-perturbative crossover regime of QCD increases the pressure of the postmerger remnant. This leads to a longer duration of the late time gravitational radiation such that the GW emission might become a means to probe the non-perturbative regime of quark matter.

In particular, in Ref. [1] various parameterizations of the quark-hadron crossover (QHC19) EOS of [41] were investigated. A complementary study has also been made in Ref. [42] based upon the newer (QHC21) version with similar conclusions. As the density increases, a critical point is thought to appear. Above that density a weak first-order chiral transition may occur [43]. In the QHC19 EOS the transition from hadronic to quark matter is treated as a continuous crossover parameterized with a 5th order polynomial. The observational constraints on the NS mass ( $> 2 M_{\odot}$ ) [44–46] and the radius bounds from the LIGO-Virgo analysis are satisfied in all versions of this EOS.

Within this context the tidal deformability, maximum chirp frequency  $f_{max}$ , and power spectral density frequency peak  $f_{peak}$  were analyzed in [1] as a means to identify observational signatures of the crossover to quark matter during binary NS mergers. The crucial postmerger GW emission occurs in a high frequency range (1–4 kHz). Although this frequency is outside the current LIGO/aVirgo/KAGRA window, it is anticipated that next generation of GW observatories such as the Einstein Telescope [47] and the Cosmic Explorer [48] will be sensitive in this frequency range. We argue that observations of such higher frequency gravitational wave emission in the next generation detectors may have the possibility to characterize both the order of the transition and the physics of the crossover regime of quark matter.

## 2 Equations of state

At high baryon density and chemical potential the QCD strong coupling  $\alpha_s$  approaches unity. A non-perturbative approach to QCD is then necessary to describe the generation of constituent quark masses, chiral symmetry breaking [49], quark pairing, and color superconductivity [50], etc. For our studies we utilized various parameterizations of the QHC19 EOS [41]. In that work, the low-density hadronic regime (i.e. less than twice the nuclear saturation density,  $< 2 n_0$ ) utilized the Togashi EOS [51, 52]. This is an extended version of the

relatively soft APR EoS [53]. Our study [1] instead utilized the SLy [54] and the GNH3 [55] EoSs as bracketing the physics of a soft and stiff EoS, respectively.

The QHC19 EOS accounts for the non-perturbative QCD effects in the context of the Nambu-Jona-Lasinio model (see Refs. [56–58]). The Lagrangian contains four coupling constants. These are: 1) the scalar coupling ( $G$ ); 2) the coefficient of the Kobayashi-Maskawa–t Hooft vertex ( $K$ ); 3) the vector coupling for universal quark repulsion ( $g_v$ ); and 4) the diquark strength ( $H$ ). In the QHC19 EoS, only two coupling constants ( $g_v$  and  $H$ , scaled to  $G$ ) are varied to construct versions of the model. The matter pressure increases as these couplings increase [40, 41]. In [1] we utilized three parameter sets from [41], identified as QHC19B [ $(g_v, H) = (0.8, 1.49)$ ], QHC19C [ $(g_v, H) = (1.0, 1.55)$ ], and QHC19D [ $(g_v, H) = (1.2, 1.61)$ ]. The pressure in the crossover regime ( $2 n_0 < n < 5 n_0$ ) is given analytically with fifth-order polynomials in terms of the baryonic chemical potential. The tidal deformability ( $\Lambda < 800$  for  $M_0 = 1.4 M_\odot$ ) [4], the maximum mass [44–46], and radius of neutron stars are all satisfied with these parameterizations of the QHC19 EOS. For numerical speed we implemented the QHC19 EOSs using piecewise-polytropic fits as described by Ref. [59] and modified as discussed in [1].

### 3 Simulations

In [1] binary merger simulations were evolved using the numerical relativity software platform, the Einstein Toolkit (ET) [60]. This platform incorporates full general relativity in three spatial dimensions based upon the BSSN-NOK formalism [61–65]. The hydrodynamics was evolved with the use of the GRHydro code [66–68] based on the Valencia formulation [69, 70]. The initial conditions were generated using LORENE [71, 72]. The thorn Carpet [73, 74] was used for adaptive mesh refinement based upon six mesh refinement levels and a minimum grid of 0.3125 in Cactus units ( $\approx 461$  m). The thermal pressure component was implemented in GRHydro using a constant adiabatic index  $\Gamma_{\text{th}} = 1.8$  as in Ref. [75].

The GWs emitted during the binary merger were extracted using the Newman-Penrose formalism which is based upon a multipole expansion of the spin-weighted spherical harmonics of the Weyl scalar  $\Psi_4^{(l,m)}(\theta, \phi, t) = \ddot{h}_+^{(l,m)}(\theta, \phi, t) + i\dot{h}_\times^{(l,m)}(\theta, \phi, t)$ . The two polarizations of the strain  $h_+(\theta, \phi, t)$  and  $h_\times(\theta, \phi, t)$  were calculated by summing over the  $(l, m)$  modes and integrated twice. The isolated NS models involved baryonic masses of  $M_B = 1.45, 1.50, 1.55 M_\odot$ , with similar gravitational masses  $\sim 1.35 - 1.4$ . These were placed on the grid with an initial coordinate separation between centers of 45 km.

Figure 1 (from Ref. [1]) illustrates the evolution of the maximum density during the simulations. This figure shows that the densities in the NSs even before the merger are well into the crossover range ( $2-5 n_0$ ). The NS core densities remain in the crossover domain at a densities of about  $n \sim 2.95 - 3.15 n_0$  during the approach to merger. Subsequently, the maximum density rises until the maximum density exceeds  $\sim 5 - 6 n_0$ . At this point the core of the system collapses to the central black hole as evidenced by a density spike in this figure.

Figure 2 illustrates the evolution of the strain for various equations of state as labelled, but for nearly identical initial conditions. The striking feature is that the GW signal endures for a much longer time for the cases with a QHC EOS. Moreover, the larger the quark coupling, i.e. going from QHCB to QHCC, the longer the duration of the postmerger GW emission. This suggests that one might learn the strength of the non-perturbative quark-matter couplings from the observation of an extended post merger phase.

Indeed, the postmerger duration, i.e., the lifetime of the hyper-massive neutron star (HMNS), strongly depends on the EOS stiffness at the crossover densities. When densities in excess of the nuclear saturation density are achieved in the core for the hadronic EOSs

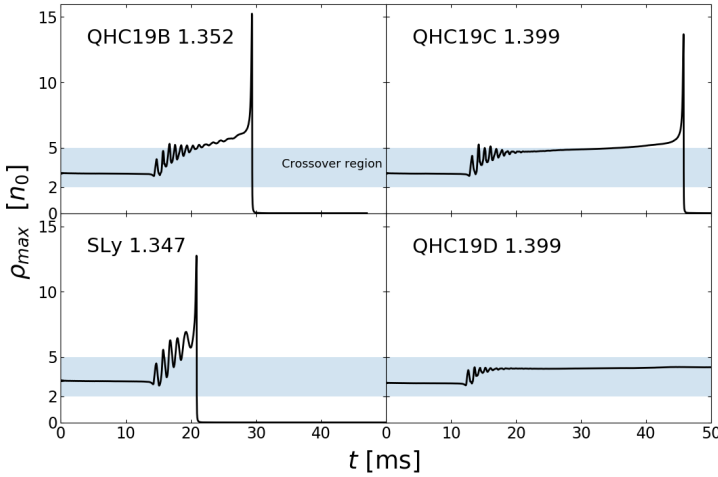


Figure 1: Evolution of maximum rest-mass density vs time for several equations of state from [1]. Numbers next to the EOS label indicate the gravitational mass of an isolated neutron star for each case. The blue band indicates QHC-crossover densities. In all cases, the NSs start in the crossover density range ( $2\text{--}5 n_0$ ) followed by a rise in density, leading to a collapse to a black hole (in all except the bottom-right panel). The bottom-right case (QHC19D 1.399) does not form a black hole within the simulation time.

it is impossible to stop the merger remnant from collapsing into a black hole. The postmerger remnants from binaries based upon the QHC19 EOS, however, have sufficient pressure to delay gravitational collapse. As the EOS stiffness within the QHC models increases, longer lifetimes of their HMNS remnants are apparent. Even the QHC19B EOS produces a much longer postmerger duration than the hadronic EOSs. For the case of QHC19D, even the highest-mass case fails to collapse.

Of course, what is actually detected in GW observatories is not the strain, but its fourier transform. In particular, an effective fourier amplitude can be deduced

$$\tilde{h}_{+, \times}(f) = \int h_{+, \times}(t) e^{-i2\pi ft} dt, \quad (1)$$

This is usually plotted as a normalized power spectral density (PSD) given by  $2\tilde{h}(f)f^{1/2}$  [76]. Figure 3 shows some PSD spectra deduced from the simulations in Ref. [1]. The upper green curve shows the LIGO sensitivity while the lower blue and orange curves show the expected sensitivity of the future Einstein Telescope and Cosmic Explorer, respectively. The first peak at around 1 kHz for all of the simulations corresponds to the initial contact of the merging neutron stars, while the second peak near 2 kHz corresponds to the maximum chirp strain,  $f_{max} = \frac{1}{2\pi} \frac{d\phi}{dt} |_{max}$ , where  $\phi$  is the phase of the strain (see [76]). Of particular interest for probing quark matter, however, is the third peak,  $f_{peak}$ , at around 3 kHz corresponding to the long postmerger phase. What can be noted in this figure is that the amplitude of  $f_{peak}$  directly correlates with the duration of the postmerger system, and therefore, relates to the strength of the coupling constants in the QHC19 EOS parameterizations.

In spite of the promising feature that  $f_{peak}$  PSD becomes large for a crossover to quark matter, it is possible that other equations of state can lead to such a peak [76]. What is

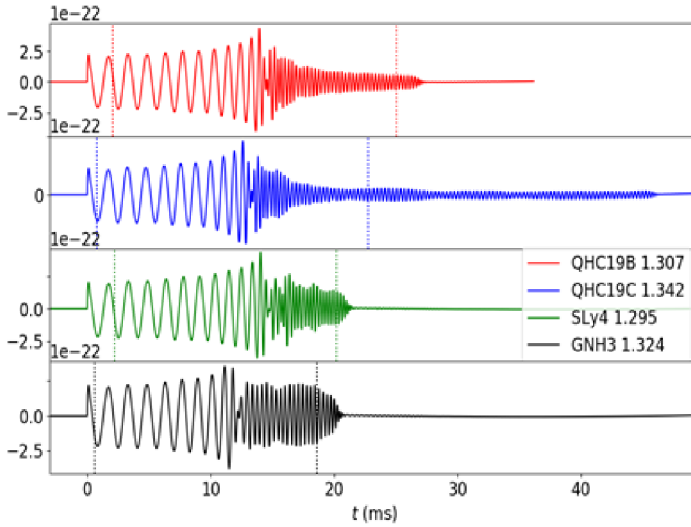


Figure 2: Evolution of the GW strain  $h_{+,x}$  vs time for several representative simulations with nearly identical starting conditions, but for different equations of state as labelled. The numbers indicate the isolated neutron star mass for each EOS as indicative of the similarity of initial conditions. The upper two curves are for parameterizations of the QHC19 EOS, while the bottom two curves are for a soft and stiff pure hadronic EOS. Note the the signal continues for a much longer duration in the cases with a crossover to quark matter.

needed, therefore, is another unique signature to specifically identify quark matter. In [1] it was suggested that the softness of the QHC equations of state at lower densities,  $\sim 3n_0$ , is apparent in their pre-merger  $f_{max}$  frequency, whereas the stiffness at higher densities is indicated in the postmerger  $f_{peak}$  frequency.

This dual nature of the QHC equations of state (having both softness and stiffness) might be revealed by observations of both  $f_{max}$  and  $f_{peak}$  in a single GW event. This is illustrated in figure 4 from Ref. [1]. The upper panel shows that the QHC equations of state in our simulations obey the scaling relations with tidal deformability as noted in [77]. This also shows that the QHC simulations all cluster with a soft EOS like the SLy in the initial chirp. However, the lower panel shows the relation between  $f_{peak}$  and the pseudo-averaged rest-mass density. Such a correlation was suggested in Refs. [25, 76]. This figure shows that in the later 3 kHz post-merger phase, the  $f_{peak}$  frequencies cluster somewhere between a soft and stiff EOS. Hence, observing such a transition in the PSD between soft to stiffness, as evidenced in the different behaviors of  $f_{max}$  and  $f_{peak}$ , may indicate the formation of quark matter. Once the existence of quark matter is confirmed the amplitude of the PSD at  $f_{peak}$  might be suggestive the strength of the quark couplings.

## 4 Acknowledgements

Work at the Center for Astrophysics of the University of Notre Dame is supported by the U.S. Department of Energy under Nuclear Theory Grant No. DE-FG02-95-ER40934. This research was supported in part by the Notre Dame Center for Research Computing through the high performance computing resources. H.I.K. graciously thanks Jinho Kim and Chunglee

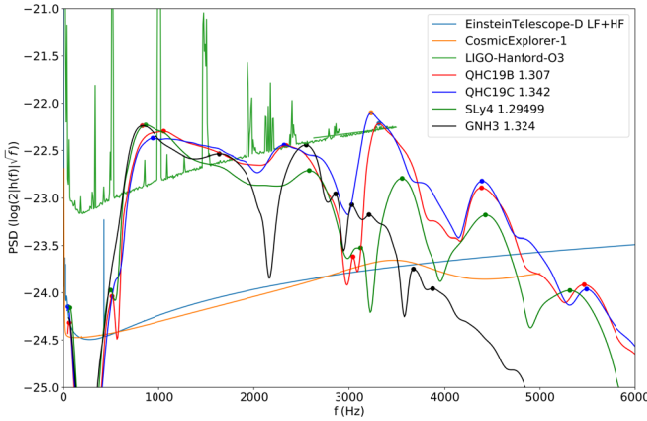


Figure 3: Power spectral density ( $2\tilde{h}(f)f^{1/2}$ ) as a function of frequency for various simulations as labelled and shown on Figure 2. The upper green curve shows the LIGO sensitivity while the lower blue and orange curves show anticipated sensitivity of the Einstein Telescope and Cosmic Explorer, respectively. The first peak at around 1 kHz for all of the simulations corresponds to the initial contact of the merging binaries. The second peak near 2 kHz corresponds to the maximum chirp strain,  $f_{max}$ , while the third peak, at around 3 kHz corresponds to the long postmerger phase,  $f_{peak}$ .

Kim for continuous support. The work of H.I.K. was supported by Basic Science Research Program through the National Research Foundation of Korea (NRF) funded by the Ministry of Education through the Center for Quantum Spacetime (CQUeST) of Sogang University (Grant No. NRF-2020R1A6A1A03047877). This research used resources of the Oak Ridge Leadership Computing Facility at the Oak Ridge National Laboratory, which is supported by the Office of Science of the U.S. Department of Energy under Contract No. DE-AC05-00OR22725.

Software used was as follows The Einstein Toolkit (Ref. [60]; <https://einsteintoolkit.org>), LORENE (Refs. [71, 72]), PyCactus (<https://bitbucket.org/GravityPR/pycactus>), and TOVsolver (<https://github.com/amotornenko/TOVsolver>).

## References

- [1] A. Kedia, H.I. Kim, I.S. Suh, G.J. Mathews, arXiv e-prints arXiv:2203.05461 (2022), 2203.05461
- [2] L. Baiotti, Progress in Particle and Nuclear Physics **109**, 103714 (2019), 1907.08534
- [3] D. Radice, S. Bernuzzi, A. Perego, Annual Review of Nuclear and Particle Science **70**, 95 (2020), 2002.03863
- [4] B.P. Abbott, R. Abbott, T.D. Abbott, F. Acernese, K. Ackley, C. Adams, T. Adams, P. Addesso, R.X. Adhikari, V.B. Adya et al., Physical Review Letters **119**, 161101 (2017), 1710.05832
- [5] B.P. Abbott, R. Abbott, T.D. Abbott, F. Acernese, K. Ackley, C. Adams, T. Adams, P. Addesso, R.X. Adhikari, V.B. Adya et al., Physical Review Letters **121**, 161101 (2018), 1805.11581

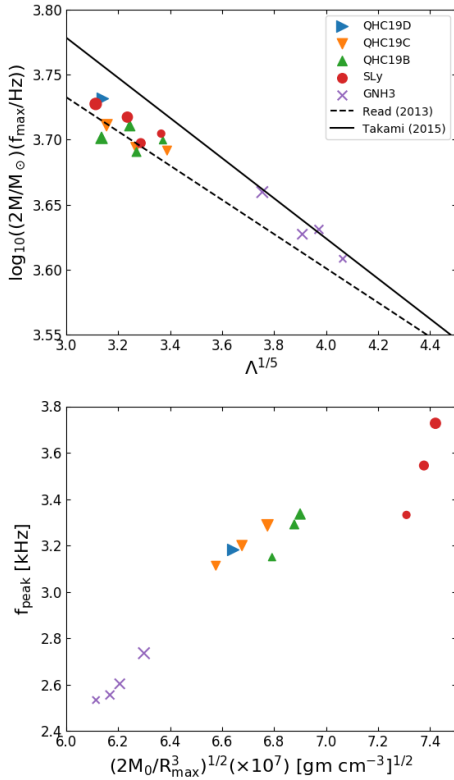


Figure 4: From Ref. [1]. Top panel shows  $f_{max}$  vs. the dimensionless tidal deformability ( $\Lambda^{1/5}$ ). Also plotted are universality relations suggested in previous work [76, 77] as indicated. The lower panel shows  $f_{peak}$  vs. the pseudo-average rest-mass density  $(2M_0/R_{max}^3)^{1/2}$ . The size of the symbols indicates the size of the gravitational mass in isolation  $M_0$  as listed in [1].

[6] J.M. Lattimer, Annual Review of Nuclear and Particle Science **62**, 485 (2012), 1305.3510  
 [7] S. Bogdanov, S. Guillot, P.S. Ray, M.T. Wolff, D. Chakrabarty, W.C.G. Ho, M. Kerr, F.K. Lamb, A. Lommen, R.M. Ludlam et al., Astrophysical Journal Letters **887**, L25 (2019), 1912.05706  
 [8] S. Bogdanov, A.J. Dittmann, W.C.G. Ho, F.K. Lamb, S. Mahmoodifar, M.C. Miller, S.M. Morsink, T.E. Riley, T.E. Strohmayer, A.L. Watts et al., Astrophysical Journal Letters **914**, L15 (2021), 2104.06928  
 [9] M.C. Miller, F.K. Lamb, A.J. Dittmann, S. Bogdanov, Z. Arzoumanian, K.C. Gendreau, S. Guillot, W.C.G. Ho, J.M. Lattimer, M. Loewenstein et al., Astrophysical Journal Letters **918**, L28 (2021), 2105.06979  
 [10] É.É. Flanagan, T. Hinderer, Physical Review D **77**, 021502 (2008), 0709.1915  
 [11] T. Hinderer, Astrophysical Journal **677**, 1216 (2008), 0711.2420  
 [12] J.S. Read, C. Markakis, M. Shibata, K. Uryū, J.D.E. Creighton, J.L. Friedman, Physical Review D **79**, 124033 (2009), 0901.3258

- [13] E.R. Most, L.R. Weih, L. Rezzolla, J. Schaffner-Bielich, *Physical Review Letters* **120**, 261103 (2018), 1803.00549
- [14] E. Annala, T. Gorda, A. Kurkela, A. Vuorinen, *Physical Review Letters* **120**, 172703 (2018), 1711.02644
- [15] A. Kurkela, P. Romatschke, A. Vuorinen, *Physical Review D* **81**, 105021 (2010), 0912.1856
- [16] O. Komoltsev, A. Kurkela, *Physical Review Letters* **128**, 202701 (2022), 2111.05350
- [17] Y. Fujimoto, K. Fukushima, Y. Hidaka, A. Hiraguchi, K. Iida, *Physics Letters B* **835**, 137524 (2022), 2109.06799
- [18] T. Gorda, O. Komoltsev, A. Kurkela, *arXiv e-prints arXiv:2204.11877* (2022), 2204.11877
- [19] S. Tootle, C. Ecker, K. Topolski, T. Demircik, M. Järvinen, L. Rezzolla, *arXiv e-prints arXiv:2205.05691* (2022), 2205.05691
- [20] L.R. Weih, M. Hanauske, L. Rezzolla, *Physical Review Letters* **124**, 171103 (2020), 1912.09340
- [21] A. Bauswein, N.U.F. Bastian, D.B. Blaschke, K. Chatziioannou, J.A. Clark, T. Fischer, M. Oertel, *Physical Review Letters* **122**, 061102 (2019), 1809.01116
- [22] S. Blacker, N.U.F. Bastian, A. Bauswein, D.B. Blaschke, T. Fischer, M. Oertel, T. Soulтанis, S. Typel, *Physical Review D* **102**, 123023 (2020), 2006.03789
- [23] D. Radice, *Astrophysical Journal Letters* **838**, L2 (2017), 1703.02046
- [24] M. Breschi, S. Bernuzzi, F. Zappa, M. Agathos, A. Perego, D. Radice, A. Nagar, *Physical Review D* **100**, 104029 (2019), 1908.11418
- [25] A. Bauswein, H.T. Janka, *Physical Review Letters* **108**, 011101 (2012), 1106.1616
- [26] K. Hotokezaka, K. Kiuchi, K. Kyutoku, T. Muranushi, Y.i. Sekiguchi, M. Shibata, K. Taniguchi, *Physical Review D* **88**, 044026 (2013), 1307.5888
- [27] S. Bernuzzi, A. Nagar, S. Balmelli, T. Dietrich, M. Ujevic, *Physical Review Letters* **112**, 201101 (2014), 1402.6244
- [28] L. Rezzolla, K. Takami, *Physical Review D* **93**, 124051 (2016), 1604.00246
- [29] F. Zappa, S. Bernuzzi, D. Radice, A. Perego, T. Dietrich, *Physical Review Letters* **120**, 111101 (2018), 1712.04267
- [30] E.R. Most, L.J. Papenfort, V. Dexheimer, M. Hanauske, S. Schramm, H. Stöcker, L. Rezzolla, *Physical Review Letters* **122**, 061101 (2019), 1807.03684
- [31] E.R. Most, L. Jens Papenfort, V. Dexheimer, M. Hanauske, H. Stoecker, L. Rezzolla, *European Physical Journal A* **56**, 59 (2020), 1910.13893
- [32] S.L. Liebling, C. Palenzuela, L. Lehner, *Classical and Quantum Gravity* **38**, 115007 (2021), 2010.12567
- [33] A. Prakash, D. Radice, D. Logoteta, A. Perego, V. Nedora, I. Bombaci, R. Kashyap, S. Bernuzzi, A. Endrizzi, *Physical Review D* **104**, 083029 (2021), 2106.07885
- [34] A. Bauswein, H.T. Janka, K. Hebeler, A. Schwenk, *Physical Review D* **86**, 063001 (2012), 1204.1888
- [35] A. Bauswein, S. Blacker, V. Vijayan, N. Stergioulas, K. Chatziioannou, J.A. Clark, N.U.F. Bastian, D.B. Blaschke, M. Cierniak, T. Fischer, *Physical Review Letters* **125**, 141103 (2020), 2004.00846
- [36] R.D. Pisarski, V.V. Skokov, *Physical Review D* **94**, 034015 (2016), 1604.00022
- [37] J. Steinheimer, S. Schramm, *Physics Letters B* **696**, 257 (2011), 1005.1176
- [38] T. Hatsuda, M. Tachibana, N. Yamamoto, G. Baym, *Physical Review Letters* **97**, 122001 (2006), hep-ph/0605018



- [39] Y. Aoki, G. Endrődi, Z. Fodor, S.D. Katz, K.K. Szabó, *Nature* **443**, 675 (2006), [hep-lat/0611014](#)
- [40] G. Baym, T. Hatsuda, T. Kojo, P.D. Powell, Y. Song, T. Takatsuka, *Reports on Progress in Physics* **81**, 056902 (2018), [1707.04966](#)
- [41] G. Baym, S. Furusawa, T. Hatsuda, T. Kojo, H. Togashi, *Astrophysical Journal* **885**, 42 (2019), [1903.08963](#)
- [42] T. Kojo, G. Baym, T. Hatsuda, *Astrophysical Journal* **934**, 46 (2022), [2111.11919](#)
- [43] A.S. Kronfeld, *Annual Review of Nuclear and Particle Science* **62**, 265 (2012), [1203.1204](#)
- [44] P.B. Demorest, T. Pennucci, S.M. Ransom, M.S.E. Roberts, J.W.T. Hessels, *Nature* **467**, 1081 (2010), [1010.5788](#)
- [45] J. Antoniadis, P.C.C. Freire, N. Wex, T.M. Tauris, R.S. Lynch, M.H. van Kerkwijk, M. Kramer, C. Bassa, V.S. Dhillon, T. Driebe et al., *Science* **340**, 448 (2013), [1304.6875](#)
- [46] E. Fonseca, H.T. Cromartie, T.T. Pennucci, P.S. Ray, A.Y. Kirichenko, S.M. Ransom, P.B. Demorest, I.H. Stairs, Z. Arzoumanian, L. Guillemot et al., *Astrophysical Journal Letters* **915**, L12 (2021), [2104.00880](#)
- [47] B. Sathyaprakash, M. Abernathy, F. Acernese, P. Ajith, B. Allen, P. Amaro-Seoane, N. Andersson, S. Aoudia, K. Arun, P. Astone et al., *Classical and Quantum Gravity* **29**, 124013 (2012), [1206.0331](#)
- [48] B.P. Abbott, R. Abbott, T.D. Abbott, M.R. Abernathy, K. Ackley, C. Adams, P. Addesso, R.X. Adhikari, V.B. Adya, C. Affeldt et al., *Classical and Quantum Gravity* **34**, 044001 (2017), [1607.08697](#)
- [49] T. Hatsuda, T. Kunihiro, *Physics Reports* **247**, 221 (1994), [hep-ph/9401310](#)
- [50] M.G. Alford, A. Schmitt, K. Rajagopal, T. Schäfer, *Reviews of Modern Physics* **80**, 1455 (2008), [0709.4635](#)
- [51] H. Togashi, M. Takano, *Nuclear Physics A* **902**, 53 (2013), [1302.4261](#)
- [52] H. Togashi, K. Nakazato, Y. Takehara, S. Yamamuro, H. Suzuki, M. Takano, *Nuclear Physics A* **961**, 78 (2017), [1702.05324](#)
- [53] A. Akmal, V.R. Pandharipande, D.G. Ravenhall, *Physical Review C* **58**, 1804 (1998), [nucl-th/9804027](#)
- [54] E. Chabanat, P. Bonche, P. Haensel, J. Meyer, R. Schaeffer, *Nuclear Physics A* **635**, 231 (1998)
- [55] N.K. Glendenning, *Astrophysical Journal* **293**, 470 (1985)
- [56] Y. Nambu, G. Jona-Lasinio, *Physical Review* **122**, 345 (1961)
- [57] Y. Nambu, G. Jona-Lasinio, *Physical Review* **124**, 246 (1961)
- [58] M. Buballa, *Physics Reports* **407**, 205 (2005), [hep-ph/0402234](#)
- [59] J.S. Read, B.D. Lackey, B.J. Owen, J.L. Friedman, *Physical Review D* **79**, 124032 (2009), [0812.2163](#)
- [60] Z. Etienne, S.R. Brandt, P. Diener, W.E. Gabella, M. Gracia-Linares, R. Haas, A. Kedia, M. Alcubierre, D. Alic, G. Allen et al., *The Einstein Toolkit*, Zenodo (2021)
- [61] T. Nakamura, K. Oohara, Y. Kojima, *Progress of Theoretical Physics Supplement* **90**, 1 (1987)
- [62] M. Shibata, T. Nakamura, *Physical Review D* **52**, 5428 (1995)
- [63] T.W. Baumgarte, S.L. Shapiro, *Physical Review D* **59**, 024007 (1998), [gr-qc/9810065](#)
- [64] M. Alcubierre, B. Brügmann, T. Dramlitsch, J.A. Font, P. Papadopoulos, E. Seidel, N. Stergioulas, R. Takahashi, *Physical Review D* **62**, 044034 (2000), [gr-qc/0003071](#)

- [65] M. Alcubierre, B. Brügmann, P. Diener, M. Koppitz, D. Pollney, E. Seidel, R. Takahashi, *Physical Review D* **67**, 084023 (2003), [gr-qc/0206072](#)
- [66] L. Baiotti, I. Hawke, P.J. Montero, F. Löffler, L. Rezzolla, N. Stergioulas, J.A. Font, E. Seidel, *Physical Review D* **71**, 024035 (2005), [gr-qc/0403029](#)
- [67] I. Hawke, F. Löffler, A. Nerozzi, *Physical Review D* **71**, 104006 (2005), [gr-qc/0501054](#)
- [68] P. Mösta, B.C. Mundim, J.A. Faber, R. Haas, S.C. Noble, T. Bode, F. Löffler, C.D. Ott, C. Reisswig, E. Schnetter, *Classical and Quantum Gravity* **31**, 015005 (2014), [1304.5544](#)
- [69] F. Banyuls, J.A. Font, J.M. Ibáñez, J.M. Martí, J.A. Miralles, *Astrophysical Journal* **476**, 221 (1997)
- [70] J.A. Font, *Living Reviews in Relativity* **11**, 7 (2008)
- [71] E.ourgoulhon, P. Grandclément, K. Taniguchi, J.A. Marck, S. Bonazzola, *Physical Review D* **63**, 064029 (2001), [gr-qc/0007028](#)
- [72] P. Grandclément, J. Novak, *Living Reviews in Relativity* **12**, 1 (2009), [0706.2286](#)
- [73] E. Schnetter, S.H. Hawley, I. Hawke, *Classical and Quantum Gravity* **21**, 1465 (2004), [gr-qc/0310042](#)
- [74] E. Schnetter, P. Diener, E.N. Dorband, M. Tiglio, *Classical and Quantum Gravity* **23**, S553 (2006), [gr-qc/0602104](#)
- [75] R. De Pietri, A. Feo, F. Maione, F. Löffler, *Physical Review D* **93**, 064047 (2016), [1509.08804](#)
- [76] K. Takami, L. Rezzolla, L. Baiotti, *Physical Review D* **91**, 064001 (2015), [1412.3240](#)
- [77] J.S. Read, L. Baiotti, J.D.E. Creighton, J.L. Friedman, B. Giacomazzo, K. Kyutoku, C. Markakis, L. Rezzolla, M. Shibata, K. Taniguchi, *Physical Review D* **88**, 044042 (2013), [1306.4065](#)